Supplementary Tables

Supplementary Table S1 Oligonucleotide primers used for MNase CHART-PCR, ChIP-qPCR and Nascent strand abundance assay

Primers	Sequence	Map positions (bp)	Product length (bp)
LB2 ORI	F-5' GACTGGAAACTTTTTTGTAC 3' R-5' GTGGAGGGATCTTTCTTAGACATC 3'	3937-3956 4070-4047	134
E-box	F-5' AACAGGACCCAGGCGATG 3' R-5' **CGGAATTC**CGTCTATACAGCGTGTTGC 3'	4110-4127 4240-4221	131
non-ORI LB2-P	F-5' CCCACTCCTCATCTCACCAT 3' R-5' ACGCCTGGATTCTGAATTTG 3'	1467-1486 1682-1663	216

Sequence of oligonucleotide primers and their map positions according to the human Lamin B2 (LAMB2) gene and ppv1 (TIMM 13) gene sequence (Gene bank accession no. M94363). Letters in bold are ectopic overhangs attached for introducing restriction sites (underlined sequence). MCM4 ORI primer and MCM4 non-ORI primer used in ChIP-qPCR and nascent strand abundance assay were described elsewhere as primer sets of UPR-F, UPR-R2 and EX7-F, EX7-R respectively (60).

Supplementary Table S2 Oligonucleotide primers used for RT-qPCR

Primers	Sequence	Map positions (bp)	Product length (bp)
TIMM 13	F-5' AATGGAGCAGGTGAAAGTGC 3' R-5' GAGTTGTAGGCGCGAGACAC 3'	4680-4699 5166-5147	199*****
ODC	F-5' ATGTTGCATCAGCTTTCAC 3' R-5' TCCATAGACGCCATCATTC 3'	836-854 972-954	133
GAPDH	F-5' CGACCACTTTGTCAAGCTCA 3' R-5' AGGGGTCTACATGGCAACTG 3'	1014-1033 1241-1222	228

Sequence of oligonucleotide primers used in RT-qPCR. The map positions of TIMM 13 primers are according to the human Lamin B2 (LAMB2) gene and ppv1 (TIMM 13) gene sequence (Gene bank accession no. M94363). Sequence of ODC oligonucleotide primers are designed for the map positions of *Homo sapiens* ornithine decarboxylase 1 (ODC1) mRNA (Gene bank accession no. NM_002539.1). GAPDH map position is according to the *Homo sapiens* Glyceraldehyde-3-phosphate dehydrogenase (GAPDH) mRNA sequence (Gene bank accession no. NM_002046). *****, indicates the 199 bp cDNA product excluding the introns located between the map positions of 4680 – 5166.

Supplementary Table S3 Oligonucleotide primers used for EMSA

Primers	Sequence
Consensus E-box	F-5' GGAAGCAGACCACGTGGTCTGCTTCC 3' R-5' GGAAGCAGACCACGTGGTCTGCTTCC 3'
lamin B2 E-box	F-5' GACTCTTCGTCACGTGATGCGACCGG 3' R-5' CCGGTCGCATCACGTGACGAAGAGTC 3'

Underlined sequences are core E-box element of c-Myc binding site. Upon DMS treatment the E-box was methylated (mEbox – $CA^{m}CGTG$).

Supplementary Table S4 List of human replication origins possessing E-box element

Origins			Position of E-box	
Chromosome	Begining	End	CACGTG	GTGCAC
chr1	148244302	148246331		148,246,043
chr1	148258507	148260234		148,258,749
chr1	148296747	148298101	148,296,758	
chr2	118505924	118507071		118,506,170; 118,506,630
chr2	220188829	220191429	220,189,106	
chr2	220228419	220230263	220,230,228	
chr2	220242014	220245496		220,242,849
chr2	220336089	220337258		220,336,875
chr2	220541427	220543128		220,542,648
chr2	234486579	234487948		234,486,670; 234,487,511
chr2	234740455	234741601	234,741,164	
chr5	55873281	55874378	55,873,964	55,874,102
chr5	56085418	56086517	56,086,155	
chr5	56119168	56120680		56,119,285
chr5	56241199	56242625	56,241,865	
chr5	131571851	131573644	131,573,154	
chr5	131860038	131861573		131,860,936
chr5	132025755	132026955	132,026,459; 132,026,929	132,026,573
chr5	132048184	132049426	132,049,285	132,049,280
chr5	132151529	132152659		132,151,546
chr5	141999954	142001505		142,000,152; 142,000,241; 142,000,649
chr5	142078249	142081176	142,079,020	
chr5	142176213	142178174	142,176,736	
chr6	41585098	41586734		41,585,657; 41,585,710
chr6	41599804	41601172	41,600,474	
chr6	41854596	41855697		41,854,775
chr6	74108528	74110397	74,108,933	
chr6	108711089	108712249		108,712,132

chr7	26922861	26924734	26,923,581	
chr7	26952545	26954275	26,953,152	
chr7	27056729	27057891		27,057,583
chr7	89478648	89479835		89,478,840; 89,478,887
chr7	89677540	89679141	89,678,998	89,678,067; 89,679,003
chr7	89870257	89871631	89,871,427	
chr7	90037675	90039130		90,037,749
chr7	90089748	90091313	90,089,986	
chr7	114318566	114319629		114,318,735
chr7	115760088	115761361	115,761,081	115,760,367; 115,761,295
chr7	116713437	116715501	116,714,185	
chr7	116799265	116800441		116,800,307
chr7	117025196	117026369		117,026,161
chr7	126581134	126582490	126,581,655	
chr7	126626567	126628059	126,627,342	
chr7	126698956	126700072		126,699,211
chr8	119374375	119375434		119,374,440
chr9	128878320	128879939		128,879,083
chr9	128950230	128954769		128,952,874
chr9	128982248	128985348	128,983,760	128,982,588
chr9	129022541	129024126	129,023,448	129,023,764
chr9	129125826	129127790	129,125,858; 129,125,967; 129,127,062	129,126,628; 129,127,059
chr9	129178491	129180032		129,179,811
chr9	129193266	129195682	129,194,195	
chr9	129220258	129221445	129,220,528; 129,221,431; 129,221,437	129,221,434
chr9	129253902	129256230		129,254,415; 129,254,592
chr11	64167296	64168971	64,168,011; 64,168,055	64,168,014; 64,168,190; 64,168,290
chr11	64289674	64293005	64,292,079	64,289,731; 64,289,749
chr11	64302035	64303808		64,303,658
chr11	64367486	64368648		64,368,167
chr11	64412337	64413999	64,412,385; 64,413,855	64,413,490
chr11	64438527	64439948	64,438,663	
chr11	130855483	130856606	130,855,600	
chr13	112428205	112429622	112,428,561	
chr13	112433768	112434909	112,434,155	112,434,152
chr13	112530134	112531863		112,531,306; 112,531,326
chr13	112561443	112562786	112,561,607	112,561,604
chr13	112596565	112597931		112,597,900
chr13	112606307	112607524		112,606,643
chr13	112612988	112614632	112,614,353	
chr13	112668983	112670626		112,670,006; 112,670,094; 112,670,154; 112,670,274; 112,670,314
chr13	112703946	112705845	112,704,980	112,704,506
chr13	112811287	112812598	112,811,809	
chr14	98486278	98487757		98,486,712

chr14	98724314	98725645	98,725,559	
chr14	98767316	98769158	98,767,976; 98,768,682	
chr14	98808316	98809543	98,808,531; 98,809,026; 98,809,204	
chr14	98881859	98883202		98,881,927; 98,882,652
chr15	41735285	41736157		41,735,450
chr16	47415	48530	47,904	47,901
chr16	128359	129221	128,642	
chr16	265752	267214	266,614	266,921
chr16	343083	344285	343,331	
chr16	353862	355393	354,732	
chr16	371926	373475	372,076; 372,105	
chr16	391235	392389	392,111	
chr16	458042	459289	458,769	
chr18	24064501	24065770		24,064,758
chr19	59077897	59080362	59,078,338	
chr19	59093470	59095647	59,095,085	
chr19	59174913	59178718	59,175,121	
chr19	59225201	59226338	59,225,309; 59,225,911; 59,226,173	
chr19	59340003	59341368	59,341,197	
chr19	59357776	59359107	59,357,966	
chr19	59588883	59590167		59,588,892
chr20	33520581	33521619	33,520,881	
chr20	33604647	33606279	33,605,235	
chr21	32924855	32926140		32,925,073
chr21	33314649	33316910	33,316,719; 33,315,366	33,315,223
chr21	33321658	33323457	33,321,956; 33,323,051; 33,323,141	33,321,689
chr21	33371196	33372523		33,371,847
chr21	33773906	33775426		33,774,178
chr21	39377239	39378501		39,377,748
chr22	30349689	30350809		30,349,983
chr22	30896070	30897269		30,896,185
chr22	31030409	31031414	31,030,978	31,031,026
chr22	31156785	31158209	31,157,562	
chr22	31195329	31197371		31,195,648
chr22	31366116	31367680	31,366,480	
chr22	31437500	31439348		31,438,454
chr22	31530713	31531675	31,531,538	
chrX	122624067	122625387		122,624,861
chrX	152662042	152663313		152,662,816
chrX	152689689	152691828	152,691,296	152,691,299
chrX	152704242	152705388		152,704,960
chrX	152721163	152722370	152,721,691	152,721,365
chrX	153081356	153082612	153,081,370; 153,082,247; 153,082,591	
chrX	153123710	153124807		153,124,666

chrX	153130060	153131533		153,130,742
chrX	153249941	153251354	153,250,430	
chrX	153327230	153328684	153,328,528	
chrX	153338595	153339968	153,339,920	153,339,401
chrX	153818861	153819900		153,818,886

Origins possessing E-box elements are listed and the position of E-box is denoted. The origin sequence mentioned here can be retrieved from the following URL. (http://genome.ucsc.edu/ENCODE/encode.hg17.html).

Supplementary Figure legends

Supplementary Figure S1. Flow cytometry of HEK293 cells and kinetics of Myc-ER recruitment to lamin B2 origin by Tam induction. (**A** and **B**) HEK293 cells, either arrested at G_0 (serum starvation) or serum stimulated for indicated time points were processed either for Flow cytometry to show the distribution of cells in different phases of cell cycle (**A**) or for western blotting to show the protein levels of cyclin D1, Phospho-Rb, cyclin E and GAPDH (**B**). (**C**) HEK293-MycER^{Tam} cells were induced for the indicated time points and fold DNA enrichment of c-Myc and Max over IgG control was measured by ChIP-qPCR. (**D**) qRT-PCR analysis was performed to measure the ODC and TIMM 13 transcripts by enforced expression of c-Myc. Data shown in (**C**) and (**D**) are mean ± SD of three independent experiments. The *number* sign indicates statistically significant difference at $p < 0.01$.

Supplementary Figure S2. Kinetics of pre-RC proteins recruitment at control non-ORI LB2-P region and enrichment of nascent strands at MCM4 non-ORI control region. (**A**) ChIP-qPCR analysis of HEK293 cells harvested during late G_1 and S phase was performed to show the recruitment kinetics of indicated proteins over IgG control for LB2 ORI. (**B**) ChIP-qPCR analysis HEK293 cells harvested during G_1 and S phase showed the recruitment kinetics of indicated proteins over IgG control for non-ORI LB2-P region. (**C**) Recruitment kinetics of c-Myc measured by ChIP-qPCR at different phases of HEK293 cells transfected either with Vector control or Myc shRNA. (**D)** HEK293 cells transfected either with Vector control or Myc shRNA were western blotted for protein levels of c-Myc, MCM4 and GAPDH. (**E**) The nascent DNA template of 1.0 kb and 1.5 kb were isolated from either vector control or Myc shRNA transfected HEK293 cells and subjected to qPCR with MCM4 ORI and MCM4 non-ORI primers. The values obtained were normalized with non-ORI primer amplification. Except (**D**), the data shown are mean ± SD of three independent experiments. The *asterisk* and *number* sign indicates statistically significant difference at $p < 0.05$ and $p < 0.01$ respectively.

Supplementary Figure S3. Flow cytometry and MNase CHART-PCR of HeLa cells released from mitotic arrest (M). (**A** and **B**) The raw data set showing MNase CHART-PCR analysis of HEK293 cells at different phases of cell cycle (G_0 - G_1) amplified either by LB2 ORI (**A**) or E-box (**B**) regions. The C_t values obtained were converted to DNA concentrations using the standard curve equation mentioned above of each primer and normalized for input variations. (**C** and **D**) HeLa cells either mitotic arrested (M) or released with fresh medium by mitotic shake-off procedure for the indicated time periods were processed for either to Flow cytometry analysis to show the distribution of cells in different phases of cell cycle (**C**) or for western blotting to show the protein levels of cyclin D1, Phospho-Rb, cyclin E and GAPDH (**D**). (**E**) MNase CHART-PCR analysis of mononucleosomal DNA obtained by complete MNase digestion of HeLa cells during M- G_1 progression. Data shown in (**E**) is mean ± SD of three independent experiments. The *number* sign indicates statistically significant difference at $p < 0.01$. (**A** and **B**) represents single raw data set, out of the triplicates used in MNase CHART-PCR analysis of HEK293 cells.

Supplementary Figure S4. Kinetics of acetylase recruitment and histone tail modifications at non-ORI LB2-P region. (**A** and **B)** The G_0/G_1 staged HEK293 cells were subjected to ChIP-qPCR and the fold DNA enrichment of non-ORI LB2-P region over IgG control was measured for GCN5, p300, HBO1 and TRRAP proteins (**A**) as well as for histone H3 K9Ac, H4 tetra-Ac and H3 K4me3 (**B**). (**C**) HEK293 cells either transfected with vector control or Myc shRNA were processed for western blotting to show the expression of indicated proteins. (**D**) HEK293-MycER^{Tam} cells were induced for the indicated time points and fold DNA enrichment of HBO1 and histone H4 tetra-Ac over IgG control was measured by ChIP-qPCR for E-box region. Except (**C**), data shown are mean ± SD of three independent experiments.

Supplementary Figure S5. Sequential order of molecular events at both ORI and E-box regions during early to mid G_1 phases. (**A)** Fold DNA enrichment of MLL1 over IgG control was measured by ChIP-qPCR for non-ORI LB2-P region in G_0/G_1 transiting HEK293 cells **(B** and **C**) HEK293 cells transfected with either vector control or Myc shRNA were processed for the following experiments. Cells were proceeded for ChIP-qPCR for both LB2 ORI and E-box regions to show the fold DNA enrichment of histone H3K4me3 over IgG control (**B**). Cell lysates were prepared for western blotting to show the expression of indicated proteins (**C**). (**D** and **E**) HEK293 cells progressing from early to mid G_1 were harvested at the indicated time points and ChIP-qPCR was performed for either LB2 ORI (**D**) or E-box regions (**E**) by immunoprecipitating the cell lysate with the indicated antibodies. (**F**) ChIP-qPCR was performed with MCM4 ORI primer to measure TET2 and TDG occupancy over IgG control during G_0 and G_1 phases of HEK293 cells. Except (**C**), data shown are mean ± SD of three independent experiments. The *number* sign indicates statistically significant difference at $p < 0.01$.

Supplementary Figure S6. Methylation profiling for E-box adjacent region of lamin B2 origin. Genomic DNA isolated from G_0 and early G_1 phased HEK293 cells were modified by bisulfite treatment. The lamin B2 origin region adjacent to E-box element (4217 to 4228, GenBank^{TM} accession no. M94363) was sequenced after treatment and compared with that of unmodified lamin B2 origin (before bisulfite treatment). The unmethylated cytosines (Cs) were converted to thymines (Ts) upon bisulfite treatment and marked as '+', whereas methylated Cs remained unchanged due to its resistance to such conversion. The methylated CpG is denoted by upward triangle (blue).

Supplementary Figure S1

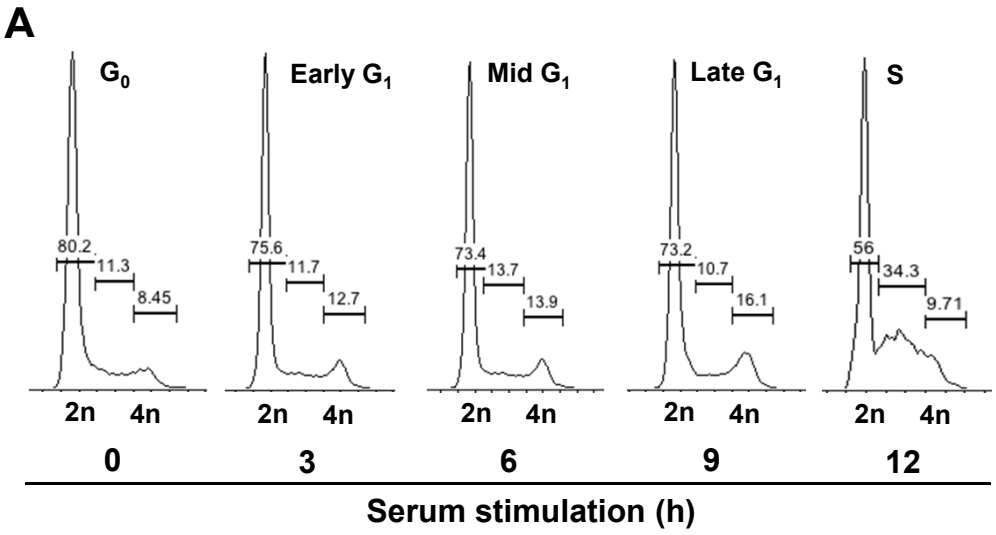

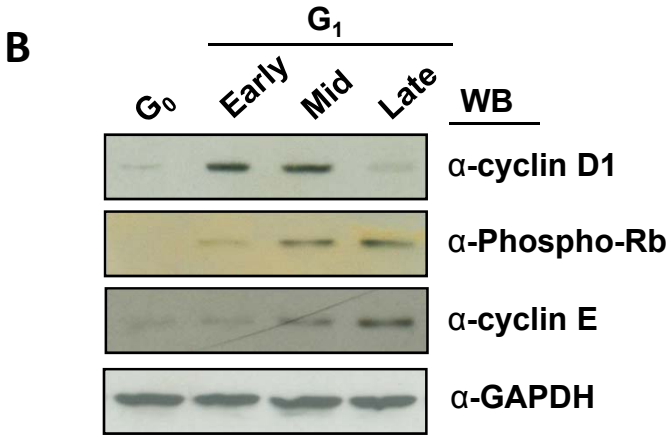

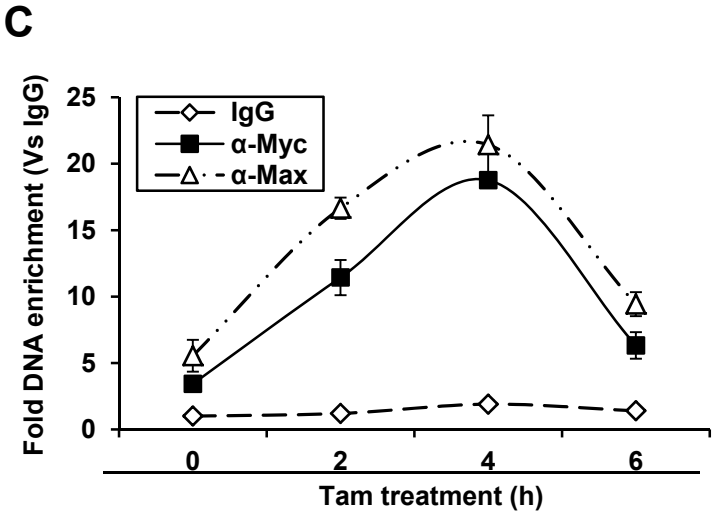

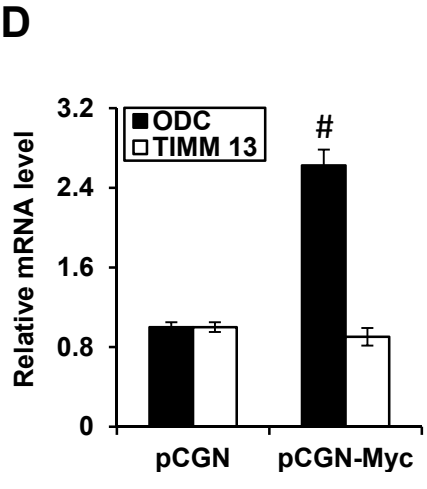

Supplementary Figure S2

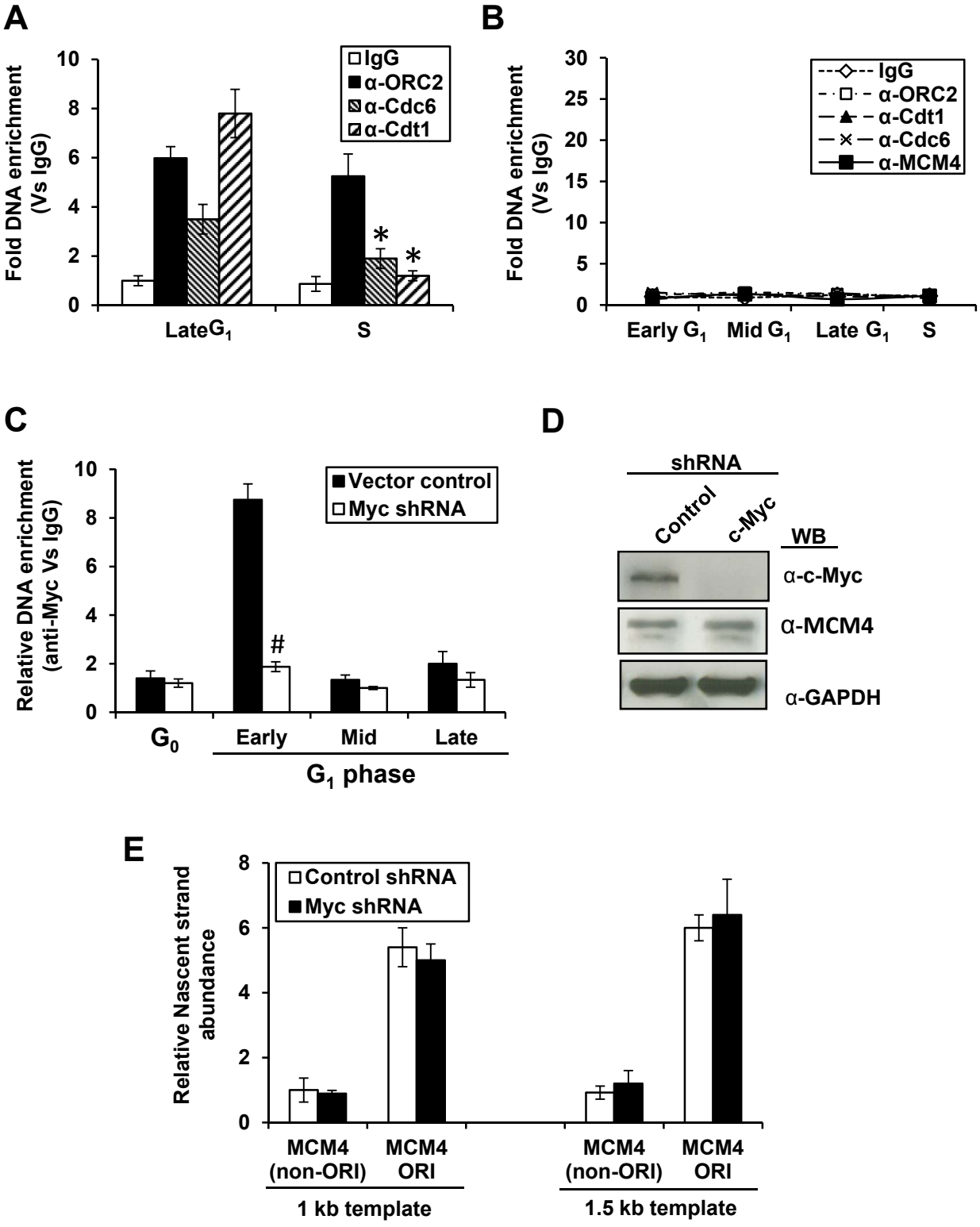

Supplementary Figure S3

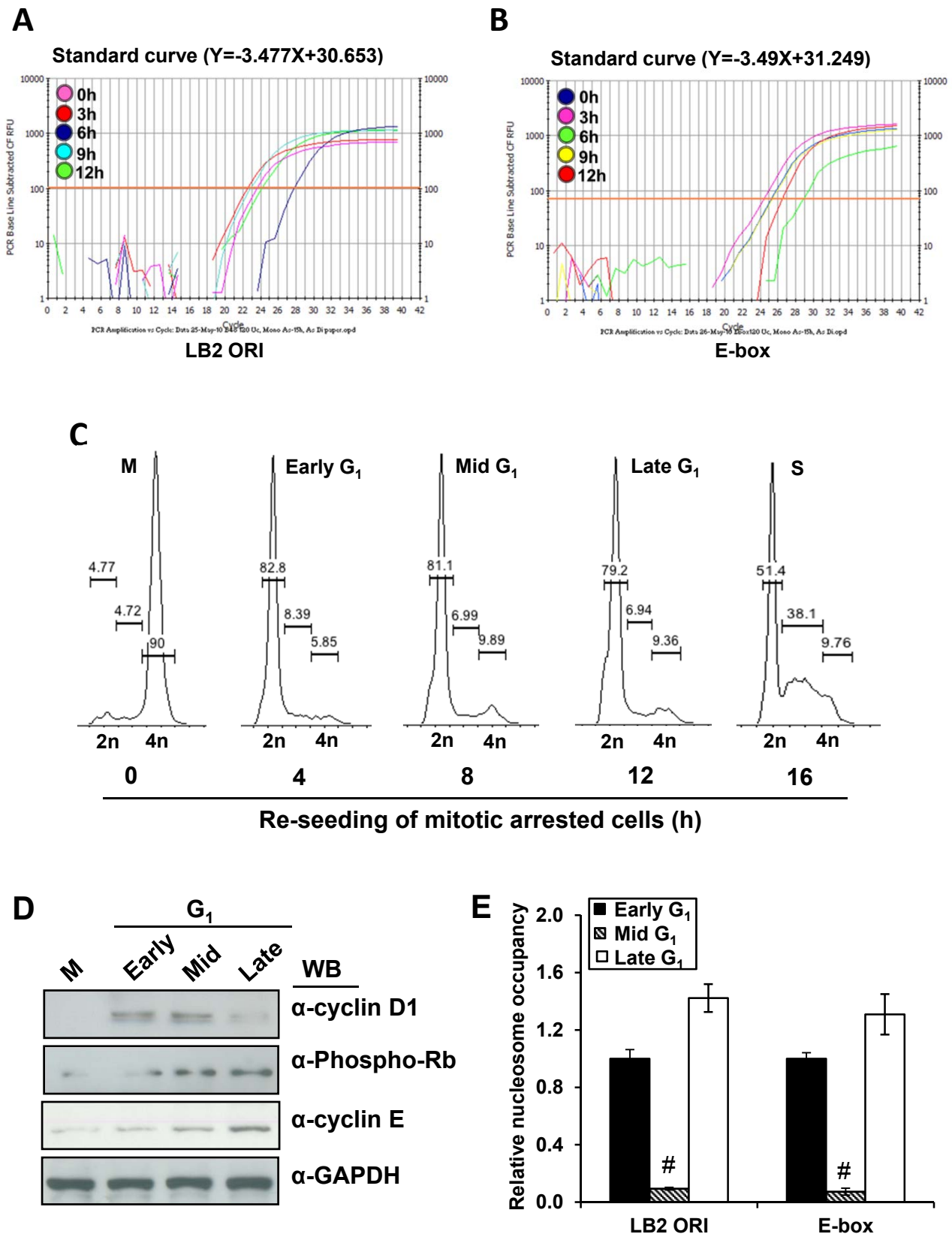

Supplementary Figure S4

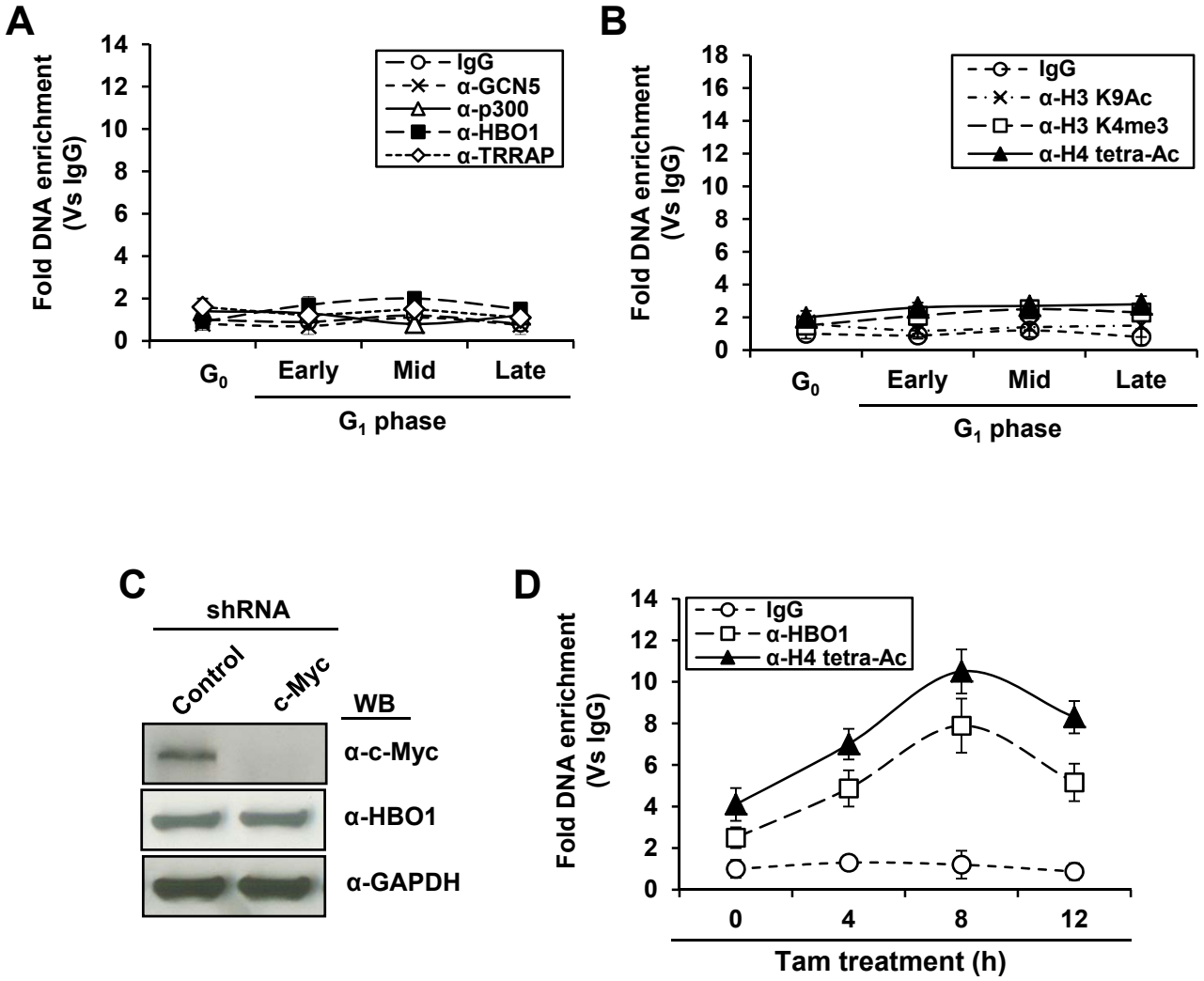

Supplementary Figure S5

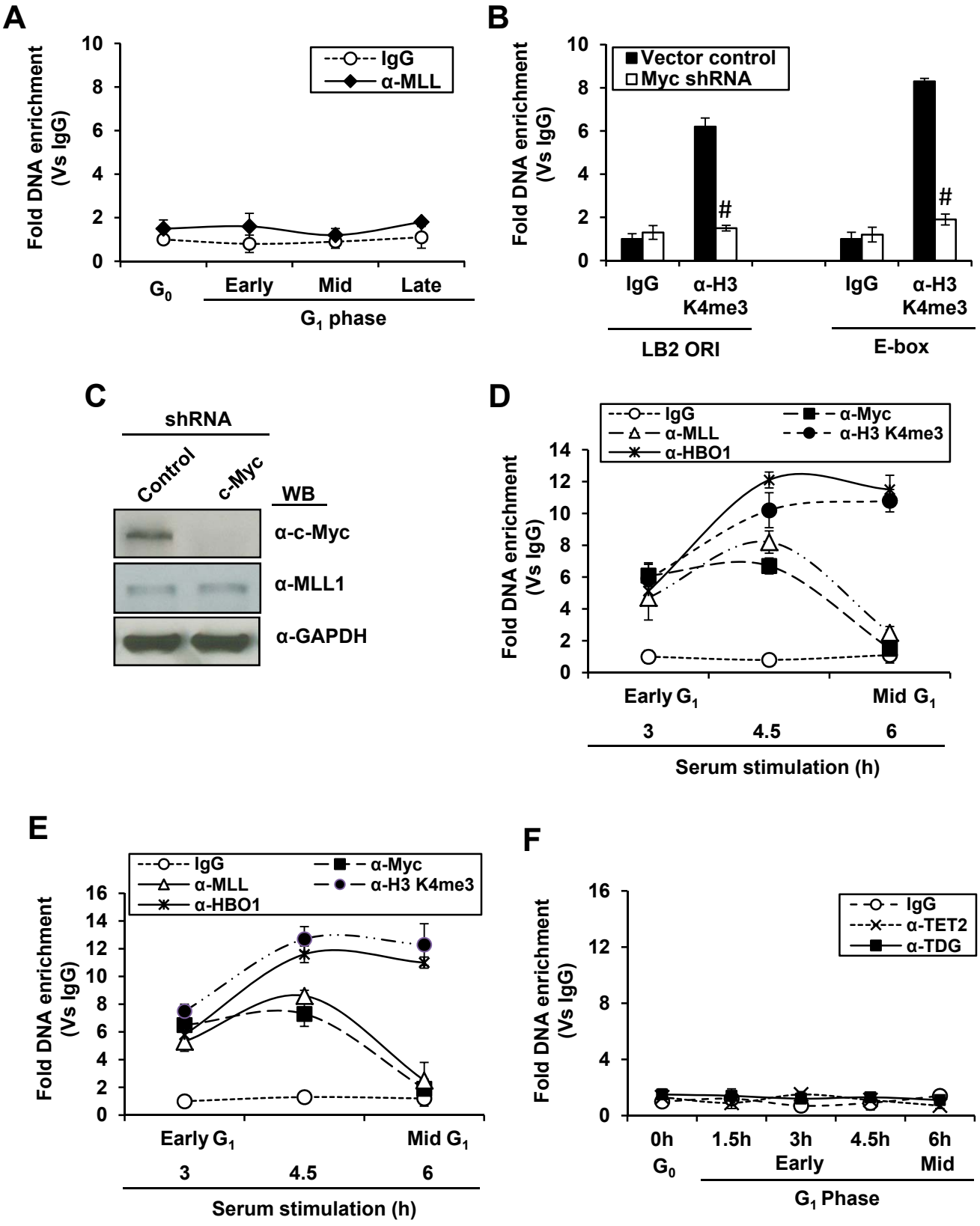

Supplementary Figure S6